Neutrophil-derived extracellular vesicles induce endothelial inflammation and damage through the transfer of miRNAs

Alexandre Glémain, Mélanie Néel, Antoine Néel, Gwennan André-Grégoire, Julie Gavard, Bernard Martinet, Rozenn Le Bloas, Kevin Riquin, Mohamed Hamidou, Fadi Fakhouri, et al.

Version of Record: https://www.sciencedirect.com/science/article/pii/S0896841122000348
Manuscript_87625d1a518d21efda449b5a9bbecbfe

Neutrophil-derived extracellular vesicles induce endothelial inflammation and damage through the transfer of miRNAs

Alexandre Glémain[1], Mélanie Néel[1], Antoine Néel[1,2], Gwennan André-Grégoire[3,4], Julie Gavard[3,4], Bernard Martinet[1], Rozenn Le Bloas[1], Kevin Riquin[1], Mohamed Hamidou[1,2], Fadi Fakhouri[1] and Sarah Bruneau[1]

[1]Nantes Université, CHU Nantes, INSERM, Center for Research in Transplantation and Translational Immunology, UMR 1064, ITUN, F-44000 Nantes, France

[2]CHU Nantes, Nantes Université, Service de Médecine Interne, Nantes, France

[3]Team SOAP, CRCI2NA, Nantes Université, Inserm UMR 1307, CNRS UMR 6075, Université d'Angers, Nantes, France

[4]Institut de Cancérologie de l'Ouest (ICO), Saint-Herblain, France

Correspondence should be addressed to: Sarah Bruneau, Centre de Recherche Translationnelle en Transplantation et Immunologie (CR2TI), INSERM UMR1064, 30 boulevard Jean Monnet, 44093 Nantes cedex 01, France. Phone: +33 (0)2 40 08 46 89 ; Fax: +33 (0)2 40 08 74 11 ; e-mail: sarah.bruneau@univ-nantes.fr

Abstract

The critical role of neutrophils in pathological inflammation, notably in various autoimmune disorders, is currently the focus of renewed interest. Here, we demonstrate for the first time that activation of neutrophils with various inflammatory stimuli induces the release of extracellular vesicles (EVs) that are internalized by endothelial cells (ECs), thus leading to the transfer of miR-223, miR-142-3p and miR-451 and subsequent endothelial damage. Indeed, while miR-223 has little effect on EC responses, we show that the induced expression of miR-142-3p and miR-451 in ECs results in profound cell damage, especially in inflammatory conditions, characterized by a dramatic increase in cell apoptosis, impaired angiogenic repair responses, and the induction of IL-6, IL-8, CXCL10 and CXCL11 expression. We show that the strong deleterious effect of miR-142-3p may be due in part to its ability to block the activation of ERK1/2 and eNOS-mediated signals in ECs. miR-142-3p also inhibits the expression of *RAC1*, *ROCK2* and *CLIC4*, three genes that are critical for EC migration and angiogenic responses. Importantly, miR-223, miR-142-3p and miR-451 are markedly increased in kidney biopsies from patients with active ANCA-associated vasculitis, a severe autoimmune disease that is prototypical of a neutrophil-induced microvascular damage. Taken together, our results suggest that miR-142-3p and miR-451 released in EVs by activated neutrophils can target EC to trigger an inflammatory cascade and induce direct vascular damage, and that therapeutic strategies based on the inhibition of these miRNAs in ECs will have implications for neutrophil-mediated inflammatory diseases.

Keywords: Neutrophils, endothelial cells, extracellular vesicles, micro-RNAs, ANCA-associated vasculitis

1. Introduction

Extracellular vesicles (EVs) are small membrane vesicles secreted by cells into surrounding biofluids that actively participate in intercellular crosstalks through the delivery to distant recipient cells of a wide range of bioactive material such as lipids, proteins, and nucleic acids, notably micro-RNAs (miRNAs) [1]. Over the past, the transfer of miRNAs through EV release and uptake has emerged as a privileged mechanism of intercellular communication between various cell types, involved not only in physiological processes such as cell adhesion, migration and differentiation [2, 3], but also in a large variety of pathological processes such as cardiovascular diseases or cancer [4, 5]. Endothelial cells (ECs) are particularly susceptible to be targeted by miRNAs released by other cell types as they are directly and continuously exposed to circulating EVs. This process has been particularly studied in cancer, where compelling evidence demonstrates that tumor cells release EVs that deliver specific miRNAs to ECs, promoting in turn tumor-associated angiogenic responses [6-9].

Neutrophils are the most abundant leukocytes in the circulation where they play an essential role in inflammation as the first effector cells recruited at the inflammatory site [10]. Like many other immune cells, neutrophils release EVs with immunoregulatory functions [11]. Interestingly, neutrophil-derived EVs have been shown to induce EC activation, characterized by IL-6 and MCP-1 secretion, as well as tissue factor induction [12, 13]. Circulating levels of neutrophil-derived EVs are markedly increased in association with several inflammatory conditions, notably in anti-neutrophil cytoplasmic antibodies (ANCA)-associated vasculitis (AAV) [14], a severe autoimmune disease that is prototypical of a neutrophil-induced endothelial cell damage [15]. Indeed, in AAV, activation of neutrophils with ANCA, autoantibodies directed against proteins expressed in their cytoplasm at resting state (typically myeloperoxidase (MPO) or proteinase 3 (PR3)), results in microvascular EC damage in various organs, in particular in lungs and kidneys. Interestingly, activation of neutrophils with ANCA *in vitro* has been found to stimulate the release of EVs that further induce ICAM-1, IL-6 and IL-8 expression in ECs, and the release of reactive oxygen species (ROS) [16]. However, the mechanisms by which these EVs can damage ECs and the pathophysiological role of the miRNAs they may contain are still unknown.

Here, we demonstrate that EVs released by neutrophils upon activation with various inflammatory stimuli, including ANCA stimulation, carry three miRNAs that are subsequently taken up by ECs, namely miR-223, miR-142-3p and miR-451. We show that, while miR-223 has little effect on EC

responses, the induced expression of miR-142-3p and miR-451 in ECs results in profound EC damage, characterized by increased cell apoptosis, impaired repair responses, and the induction of pro-inflammatory chemokines and cytokines. Importantly, these three miRNAs are increased in kidney biopsies from patients with active AAV. Collectively, our data define a new mechanism whereby neutrophils induce EC damage during inflammation through the release of miRNA-loaded EVs, and suggest that therapeutic strategies targeting miR-142-3p and miR-451 in ECs have promising implications for the treatment of AAV and other neutrophil-mediated inflammatory diseases.

2. Materials and methods

2.1. Antibodies and reagents

ANCA antibodies used in our *in vitro* neutrophil activation model were mouse monoclonal anti-MPO IgG1 (2C7 clone, Abcam) and mouse monoclonal anti-PR3 IgG1 : the CLB12.8 clone (Interchim) was initially used, but after its commercialization was discontinued another monoclonal mouse IgG1, the PR3G-2 clone (Hycult Biotech), that recognizes similar epitopes compared to the CLB12.8 [17], was used. The control isotype antibody was the mouse IgG1 clone 11711 (R&D Systems). Total IgG from two patients with active anti-PR3 ANCA-associated vasculitis were isolated from plasma samples collected following plasma exchange treatment, onto Protein A columns (GE Healthcare), according to the manufacturer's instructions. Antibodies against phosphorylated p44/42 MAPK (T202/Y204), p44/42 MAPK, phosphorylated eNOS (S1177), eNOS, and β-actin were purchased from Cell Signaling Technology. Antibodies used in confocal microscopy studies were a purified anti-CD31 antibody (Abcam), and a secondary goat AlexaFluor 488 conjugated anti-mouse IgG (H+L) antibody (Invitrogen). DAPI was from ThermoFisher Scientific. Lipopolysaccharides (LPS) from E.Coli 0111:B4 and N-Formyl-Met-Leu-Phe (fMLP) were from Sigma Aldrich. Phorbol 12-myristate 13-acetate (PMA) was purchased from InvivoGen. Human recombinant TNFα was obtained from R&D Systems.

2.2. Cell culture

Single donor primary human dermal microvascular endothelial cells (HDMEC) were purchased from Clonetics (Lonza) and cultured in complete EGM-2MV medium (Lonza). Cells were used between passages 5 to 8.

2.3. Subjects and ethics statement

Neutrophils from healthy volunteers were isolated from blood collected at the Etablissement Français du Sang (EFS, Nantes, France) with written informed consent. Plasma and neutrophils were also collected from the blood of AAV patients who gave written informed consents, and were integrated into the NALVANCA biocollection, located in the BRC of the Nantes University Hospital, under the responsibility of Dr. Néel. Each experiment was performed using a different blood donor. Residual

human biological samples were collected during the treatment of patients, with written informed consents (consent form validated by CPP Ouest IV on 07/04/2015) and the samples were integrated into the collection of human biological samples DIVAT nephro, located in the BRC of the Nantes University Hospital, under the responsibility of Dr. Giral. Plasma, neutrophils and kidney biopsy samples were integrated into the collections of human biological samples attached to the 'Immuno-transplantation" research program declared on 05/09/2011 under the n° DC-2011-1399 and in the following amending declarations (DC-2012-1555 ; DC-2013-1832 ; DC2014-2206 and DC-2017-1987 currently pending) at the Ministry of Research and having obtained a favorable decision from the CPP Ouest IV on 07/04/2015.

2.4. Neutrophil purification, activation, and EV isolation

Whole blood samples from healthy volunteers were separated on a Ficoll gradient, and the lower fraction containing red blood cells and granulocytes was gently mixed with one volume of 2% Dextran and left to sediment for 30 minutes. The supernatant containing neutrophils was collected, and after lysis of the remaining red blood cells, neutrophils were finally resuspended at $5x10^6$ cells/mL in RPMI (Gibco, Life technologies) before performing the ANCA-mediated activation protocol. Neutrophils were primed for 15 min at 37°C with 2 ng/mL TNFα to induce PR3 externalization, and further activated for 4 hours with 5 µg/mL of mouse monoclonal anti-PR3 ANCA (CLB12.8 or PR3G-2 clones, cf. figure legends), or with 200 µg/mL of total IgG purified from the plasma of patients with active anti-PR3 AAV. Alternatively, neutrophils were activated for 4 hours at 37°C with 1 µM fMLP, 20 nM PMA, or 100 ng/mL LPS. EVs released in the culture medium were collected by ultracentrifugation (see below) or using the Exoquick reagent (System Bioscience) according to the manufacturer's instructions. Their concentration and diameter were analyzed by Tunable Resistive Pulse Sensing (TRPS) using the qNano system (IZON) [18].

2.5. Assessment of EV uptake by HDMEC

EVs released by neutrophils upon *in vitro* ANCA-mediated activation were collected by ultracentrifugation. Briefly, the culture medium was centrifuged for 30 min at 10,000 g to pellet dead cells and larger particles, and the supernatant was further ultracentrifuged for 90 min at 100,000 g to

pellet EVs. These EVs were stained with the fluorescent lipophilic dye Vybrant™DiD (ThermoFisher Scientific) for 20 min at 37°C, and added to the culture medium of HDMEC (EVs released by 25 x 10^6 activated neutrophils were added to a well of a 12-well plate of confluent HDMEC) for 3 and 24 hours at 37°C. HDMEC were then washed extensively in PBS, and stained with anti-CD31 antibodies and DAPI. EV uptake was assessed by confocal microscopy on a Nikon Eclipse Ti inverted microscope and the Nikon NIS-Elements software, within the Cellular and Tissular Imaging Core Facility of Nantes University (MicroPICell). EV uptake was also evaluated by flow cytometry using a BD FACSCanto II flow cytometer and analyzed with FlowJo® 7.6.5 software (Tree Star Inc.).

2.6. miRNA profiling in HDMEC by TaqMan Low Density Arrays

HDMEC were co-incubated for 24 hrs with EVs released by ANCA-activated neutrophils (EVs from 25 x 10^6 neutrophils per well of a 12-well plate), and after extensive PBS washes, miRNA expression profiles of HDMEC were analyzed by Taqman Low Density Arrays (Applied Biosystems) according to the manufacturer's instructions. Briefly, RNA was extracted using the *mir*Vana™ miRNA Isolation kit (Invitrogen), and miRNAs were reverse transcribed using the Megaplex Primer Pools and the Taqman™ MicroRNA Reverse Transcription Kit (Applied Biosystems). After a step of preamplification of miRNAs using the Megaplex™ PreAmp Primers and the TaqMan™ PreAmp Master Mix (Applied Biosystems), miRNA profiles were analyzed using the Taqman™ Array Human MicroRNA A+B Cards set (Applied Biosystem) that enables the analysis of a selection of 754 human mature miRNAs, with a Viia™ 7 real-time PCR thermocycler (Applied Biosystems). Results obtained were validated using specific qPCR (see below).

2.7. Transfection of miRNA mimics and miRNA inhibitors

HDMEC were transfected with 10 nM of miRNA mimics (hsa-miR-223-3p, hsa-miR-142-3p, hsa-miR-451a) and a negative control miRNA mimic (Ambion, Life Technologies), or 20 nM of miRNA inhibitors or "antagomiR" (hsa-miR-142-3p and hsa-miR-451a mirVana inhibitors) and a negative control antagomiR (Ambion, Life Technologies) using Lipofectamine® RNAimax (ThermoFisher) according to the manufacturer's instructions. The overexpression efficiency was assessed 48 hours after transfection by specific qPCR.

2.8. Analysis of HDMEC apoptosis by flow cytometry

HDMEC apoptosis was assessed using the Dead Cell Apoptosis Kit with Annexin-V-FITC and Propidium Iodide for flow cytometry (Invitrogen) according to the manufacturer's instructions. The percentage of Annexin-V positive cells was analyzed using a BD FACSCanto II cytometer (BD Biosciences) and the FlowJo® 7.6.5 software (Tree Star Inc).

2.9. Analysis of HDMEC proliferation by BrdU incorporation assay

HDMEC proliferation was assessed by Bromo-deoxy-uridine (BrdU) incorporation assay using the APC BrdU Flow Kit (BD Biosciences) as per manufacturer's instructions. Briefly, HDMEC were transfected with miRNA mimics and 10 µM BrdU was added to the culture medium for the last 18 hrs of culture. HDMEC were then fixed, permeabilized, treated with 300 µg/mL DNase I, and stained with the APC-conjugated anti-BrdU antibody. The percentage of cells that had incorporated BrdU was analyzed by flow cytometry (BD FACSCanto II, BD Biosciences cytometer and FlowJo® 7.6.5 software).

2.10. Tube Formation Assay

To assess *in vitro* angiogenesis, HDMEC were collected 48 hours after miRNA mimic transfection and seeded on top of a 24-well plate (50,000 cells/well) coated with 250 µL per well of matrigel basement membrane matrix (Corning®). After 6 hours of incubation at 37°C, the network of tubes formed was observed under an inverted microscope (Olympus IX71, x4) and 4 fields of view per condition were photographed (Olympus DP72 camera and CellSens Viewer acquisition software, Olympus). Pictures were analyzed using the "Angiogenesis Analyzer" macro (Gilles Carpentier) of the Fiji® software. Results are expressed as the number of junctions measured in the capillary network.

2.11. Wound-Healing Assay

HDMEC were transfected with miRNA mimics and 48 hours later, a linear wound was created in confluent cell monolayers by scratching with a pipet tip. After an additional 24-hour incubation, cell migration into the wound was assessed by microscopy (Nikon Eclipse TS100). Four images per condition (10X magnification) were taken with a Canon G11 camera and the area of the initial wound recovered by migrating cells was measured using the Fiji® software.

2.12. Western blot

HDMEC were lysed 48 hours after miRNA mimic transfection with radioimmunoprecipitation assay (RIPA) buffer (Cell Signaling Technology) containing protease and phosphatase inhibitors (ThermoFisher Scientific). Proteins were separated on a sodium dodecyl sulfate-polyacrylamide gel and transferred onto polyvinylidene fluoride membranes. After blocking for 1 hour in PBS-0.1% Tween-20 containing 5% bovine serum albumin, membranes were incubated overnight at 4°C with primary antibodies, washed, and incubated with specific secondary peroxidase-coupled antibodies. Proteins of interest were finally detected with the SuperSignal™ West Pico Chemiluminescent Substrate (Thermo Scientific) using a LAS-400 Image Analyser (Fujifilm - LifeScience). Pictures were analyzed using the MultiGauge software (Fujifilm - Life Science). Quantification was performed using the ImageJ software, by measuring the mean gray value of each band.

2.13. Gene expression studies

Total mRNA was isolated from HDMEC 48 hours following miRNA mimic transfection using the miRNeasy isolation kit (Qiagen) and cDNA was generated using the High Capacity cDNA Reverse Transcription kit (Applied Biosystems) according to the manufacturer's instructions. A TaqMan Custom Plate designed to analyze the expression of 92 genes of interest related to endothelial cell biology (ThermoFisher Scientific, **Supplementary Table 2**) was used to examine HDMEC responses to miRNAs of interest. Results were validated by quantitative RT-PCR as described above.

2.14. Quantitative real-time PCR

Quantitative real-time PCR was performed to analyze miRNA and gene expression levels in HDMEC. For miRNA expression analyses, total RNA enriched in miRNAs was extracted from HDMEC using the *mir*Vana™ miRNA Isolation kit (ThermoFisher Scientific) according to the manufacturer's instructions. Reverse transcriptions (RT) and qPCR specific for each miRNA of interest were performed using the MicroRNA Reverse Transcription Kit (Applied Biosystems) and specific Taqman™ miRNA expression assays (Applied Biosystems). For gene expression analysis, mRNA were extracted from HDMEC using the RNeasy isolation kit (Qiagen). cDNA was generated using the High Capacity cDNA reverse transcription kit (Applied Biosystems) and qPCR was performed using specific Taqman™ gene expression assays. Relative expression of each miRNA vs. the RNU48 control, and of each mRNA vs. the HPRT control, were calculated according to the $2^{-\Delta\Delta Ct}$ method, as previously described [19].

2.15. Protein arrays

Expression of 43 human kinases and proteins in their total and phosphorylated forms was analyzed using the Proteome Profiler Human Phospho-Kinase Array Kit (R&D Systems) according to the manufacturer's instructions.

2.16. Enzyme-linked immunosorbent assays

Secretion of IL-6, IL-8, CXCL10 and CXCL11 was analyzed in culture supernatants using the specific Human DuoSet ELISA kits (R&D Systems) according to the manufacturer's instructions.

2.17. miRNA quantification in kidney biopsies

Total RNA enriched in miRNAs was isolated from human kidney biopsies using the gentleMACS™ dissociator and the mirVana™ miRNA Isolation kit (ThermoFisher Scientific), according to the manufacturer's instructions. Specific miRNA reverse transcription, preamplification and quantitative real-time PCR were performed as described above.

2.18. Statistical analysis

All data are presented as mean ± SEM. Statistical analyzes were performed using the Mann-Whitney U test or using the non-parametric ANOVA test with the Dunn's test for multiple comparisons except when mentioned, and *P* values < 0.05 were considered significant.

3. Results

3.1. Activated neutrophils release EVs that transfer miR-223, miR-142-3p and miR-451 to microvascular endothelial cells.

To study whether activated neutrophils release miRNA-loaded EVs that can damage the endothelium, we used the model of ANCA-associated vasculitis (AAV), a disease that is prototypical of an inflammatory damage of ECs induced by neutrophils. Freshly isolated neutrophils from healthy donors were primed with TNFα and further activated with anti-PR3 ANCA (clone CLB12.8) for 4 hours. EVs released in the culture supernatant were collected using the Exoquick reagent (System Biosciences) and analyzed using tunable resistive pulse sensing (TRPS, qNano, IZON). As illustrated in **Figure 1A-B**, and consistent with previous reports [14, 16], we found that activation of neutrophils with ANCA stimulated the release of EVs. Most of the EVs released upon neutrophil activation were small particles of a mean diameter below 100 nm (**Figure 1C**).

To determine whether EVs could be taken up by ECs, EVs were stained with the fluorescent lipophilic dye Vybrant DiD and co-incubated with primary cultures of human microvascular dermal endothelial cells (HDMEC). Confocal microscopy and flow cytometry analyzes showed that neutrophil-derived EVs were internalized very efficiently by 100% of HDMEC within 24 hours (**Figure 1D-E**).

To determine if the uptake of neutrophil-derived EVs by HDMEC resulted in the transfer of miRNAs carried by these EVs, we analyzed the miRNA expression profiles in HDMEC before and after 24 hours of co-incubation with these EVs, using TaqMan Low Density Arrays (TLDA, *ThermoFisher Scientific*) (**Supplementary Table 1**). We thus identified twelve miRNAs that were significantly upregulated in HDMEC after co-incubation with neutrophil-derived EVs, three of which were confirmed to be increased after a validation step by qPCR in five additional experiments, namely miR-223, miR-142-3p and miR-451 (**Figure 1F**). This miRNA transfer through EVs was also observed after activation of neutrophils with an anti-MPO antibody (**Supplementary Figure 1A**). Of note, the basal expression of these three miRNAs in resting ECs was barely detectable (Ct>30). qPCR analyzes showed that only the mature forms of these miRNAs were upregulated following co-incubation with EVs, while their

precursors (primary miRNAs or "pri-miRNAs") remained unchanged (**Figure 1F**), which strongly supports a direct transfer of these miRNAs into ECs via EVs rather than an upregulation of their biosynthesis pathways. Consistent with this observation, we found that EVs released by PR3 ANCA-activated neutrophils were loaded with miR-223, miR-142-3p and miR-451 (**Supplementary Figure 1C**). To investigate the clinical relevance of this data, neutrophils isolated from four relapsing PR3+ AAV patients were cultured for 4 hours at 37°C without additional stimulation, considering that they had already been activated *in vivo*. Secreted EVs from these cells were able to transfer miR-223, miR-142-3p and miR-451 (**Supplementary Figure 1B**). Importantly, activation of neutrophils with IgG purified from the plasma of two patients with active anti-PR3 AAV, but also activation of neutrophils with other inflammatory stimuli, *i.e.* fMLP, PMA and LPS, all resulted in the release of EVs that transferred miR-223, miR-142-3p and miR-451 to HDMEC upon co-incubation (**Figure 1G**). This suggests that the release of these three miRNAs by neutrophils and their subsequent uptake by ECs is a shared process between various inflammatory conditions.

3.2. miR-142-3p and miR-451 induce EC apoptosis and impair endothelial repair responses

We next dissected the consequences of an overexpression of miR-223, miR-142-3p and miR-451 in ECs, by transfecting HDMEC with synthetic analogues of these miRNAs ("miRNA mimics") (**Supplementary Figure 2**) vs. a negative control mimic, in the presence or the absence of TNFα, in order to reproduce a pro-inflammatory microenvironment. Phenotypically, HDMEC exhibited severe cellular damages following miR-142-3p transfection, and an elongated profile characteristic of activated ECs after miR-451 transfection (**Supplementary Figure 3**). Analysis of HDMEC apoptosis by flow cytometry using Annexin V staining showed a significant pro-apoptotic effect of miR-142-3p, which was most dramatic in the presence of TNFα ($P<0.001$) (**Figure 2A**). No overt impact on proliferation was however noted (**Figure 2B**). miR-451 overexpression also increased HDMEC apoptosis at steady state ($P<0.001$), but had little additional effect in the presence of TNFα. On the other hand, miR-451 overexpression had a moderate anti-proliferative effect in HDMEC ($P<0.05$), as assessed by BrdU incorporation assay (**Figure 2B**). To determine whether these miRNAs might interfere with EC repair and angiogenic responses, we performed *in vitro* wound-healing and tube formation assays. As illustrated in **Figure 2C**, we found that miR-142-3p completely abolished EC wound healing ($P<0.001$), which mirrors its marked pro-apoptotic effect. In contrast, miR-223

overexpression accelerated HDMEC wound healing (P<0.001), suggesting a protective effect. Besides, miR-142-3p (and miR-451, in a lesser extent) dramatically decreased HDMEC angiogenic responses *in vitro* in tube formation assays (P<0.05) (**Figure 2D**), which again probably resulted in part from its strong effect on EC apoptosis.

3.3. miR-142-3p inhibits critical genes and signaling pathways in EC

To identify intracellular signaling pathways that could be impacted by miR-223, miR-142-3p and miR-451 overexpression in EC, we performed a phospho-kinase array in order to profile the relative levels of phosphorylation of multiple kinases and some of their protein substrates in HDMEC transfected with a mix of miR-223, miR-142-3p and miR-451 mimics, in comparison with control mimic-transfected cells. As illustrated in **Supplementary Figure 4**, this array highlighted a marked inhibitory effect of these miRNAs on several signaling pathways, notably eNOS- and p44/42-MAPK (ERK1/2)-mediated signals. Additional Western blot analyzes showed that miR-142-3p strongly inhibited the induction of eNOS and ERK1/2 phosphorylation/activation upon TNFα exposure (**Figure 3A**), which may explain in part its potent deleterious effect on EC apoptosis and repair responses, especially in the presence of TNFα. In contrast, miR-223 and miR-451 had little effect on the regulation of these pathways (data not shown). Given the strong inhibitory effect of miR-142-3p on EC angiogenic repair responses, we performed in silico analysis of its predicted and/or experimentally determined direct target genes using the DianaTools and Targetscan databases (http://snf-515788.vm.okeanos.grnet.gr/ and http://www.targetscan.org/vert_72/). Genes related to cell proliferation, migration and motility, were further selected for qPCR analysis. As illustrated in **Figure 3B**, we found that miR-142-3p markedly downregulated the expression of three genes critical for EC migration and angiogenic responses [20-22], *RAC1*, *ROCK2* and *CLIC4* (P<0.05), in the presence or the absence of TNFα. Thus, beyond its potent deleterious effect on EC viability, miR-142-3p may additionally interfere with vascular repair responses through the blockade of EC migration.

3.4. miR-142-3p and miR-451 induce the expression of pro-inflammatory chemokines and cytokines by EC that may participate in EV-induced inflammation.

To identify other key genes regulated by miR-223, miR-142-3p and miR-451 in EC, we performed qPCR analysis on HDMEC transfected with each individual miRNA mimic or a negative control mimic, using custom qPCR-based arrays. Of a total of 92 genes related to EC biological responses examined in this array (**Supplementary Table 2**), we found 4 genes encoding for pro-inflammatory cytokines and chemokines that were markedly upregulated in HDMEC upon miR-142-3p and/or miR-451 overexpression. miR-142-3p overexpression induced the expression of IL-6, CXCL10 and CXCL11 (P<0.05), while miR-451 overexpression enhanced IL-8, CXCL10 and CXCL11 mRNA expression (P<0.05) (**Figure 4A**). This suggests that miR-142-3p and miR-451 overexpression in EC might participate in the induction of an inflammatory response of these cells.

Hence, we tested whether EV released by PR3 ANCA-activated neutrophils were able to induce the secretion of these cytokines and chemokines by EC. Indeed, we found that EV produced by neutrophils upon stimulation with IgG isolated from PR3-AAV patients significantly induced the secretion of IL-6 (P<0.01), IL-8 (P<0.5), CXCL10 (P<0.001), and CXCL11 (P<0.01), as compared to EV from non-stimulated (NS) neutrophils (**Figure 4B**).

To assess whether this pro-inflammatory effect of EVs resulted from the transfer of miR-142-3p and miR-451, as suggested by the series of miRNA mimic overexpression assays, HDMEC were transfected with specific miRNA inhibitors, or “AntagomiR” before co-incubation with activated neutrophil-derived EVs. 48 hours later, levels of IL-6, IL-8, CXCL10 and CXCL11 released in the culture supernatant were measured by ELISA (**Figure 4C**). Although EVs induced the release of these molecules (P<0.5, n=5) as described above, miR-142-3p and miR-451 inhibitors failed to diminish this secretion, while they efficiently prevented the induction of IL-6, IL-8, CXCL10 and CXCL11 mRNA expression upon miR-142-3p and -451 mimic transfection (data not shown). This suggests that the transfer of these miRNAs is not solely responsible for the induction of endothelial inflammation by EVs, which might exert other pro-inflammatory actions on EC.

3.5. Neutrophil-derived EVs induce EC apoptosis in a miR-142-3p-dependent manner

Because we found that miR-142-3p and miR-451 robustly trigger EC apoptosis, while miR-223 seems to have little effect on EC responses, and was even protective in wound healing assays, we next analyzed the global effect on ECs of all miRNAs transferred by neutrophil-derived EVs. To this aim,

we analyzed HDMEC apoptosis upon co-incubation with EVs released by PR3 ANCA-activated neutrophils *in vitro*. As illustrated in **Figure 5A**, EVs released by neutrophils upon PR3 ANCA-activation induced a strong increase in HDMEC apoptosis in the presence of TNFα ($P<0.01$) as compared to untreated EC and to EC treated with TNFα alone, while EVs released by resting neutrophils had no clear effect. On the other hand, EVs from activated neutrophils were unable to induce significant EC apoptosis in the absence of TNFα, suggesting that this process is dependent on the presence of an inflammatory stimuli. To evaluate whether the pro-apoptotic effect of EVs resulted from the transfer of miR-142-3p and/or miR-451, specific inhibitors of these two miRNAs ("Antagomirs") were transfected in TNFα-primed HDMEC prior to their co-incubation with neutrophil-derived EVs. As shown in **Figure 5B**, miR-142-3p inhibition markedly reduced the induction of EC apoptosis by neutrophil-derived EVs, while miR-451 inhibition had no significant impact, suggesting that miR-142-3p plays a significant role in the induction of apoptosis by neutrophil EVs.

3.6. miR-223, miR-142-3p and miR-451 are increased in kidney biopsies from patients with AAV

Finally, we analyzed the levels of expression of miR-223, miR-142-3p and miR-451 in kidney biopsies from eight patients with ANCA-associated vasculitis (**Table 1**), as compared to patients with non-proliferative glomerulonephritides (minimal change disease (n=4) and membranous nephropathy (n=1)) and to patients with other proliferative glomerulonephritides (lupus nephritis (n=5), IgA nephropathy (n=3) and membranoproliferative glomerulonephritis (n=1)) (**Table 2**). As illustrated in **Figure 6**, we found that miR-223, -142-3p and -451 were increased in AAV kidney biopsies, although their expression was not correlated with the type of ANCA involved, nor with other clinico-biological parameters. In addition, while these three miRNAs tended to be expressed at higher levels in AAV kidney biopsies as compared to proliferative glomerulonephritis control diseases, this was not statistically significant. Altogether, these results seem to be consistent with an overexpression of miR-223, -142-3p and -451 in inflammatory microvascular lesions, that seems particularly important in the context of AAV.

4. Discussion

The importance of neutrophils in the pathogenesis of numerous inflammatory diseases, including some autoimmune diseases, is increasingly recognized, and their function in pathological inflammation has recently been the focus of great interest [23, 24]. Here, using a model of ANCA-associated vasculitis, a prototype of neutrophil-mediated autoimmune vascular injury [15, 16, 25], we describe for the first time a mechanism whereby activated neutrophils induce endothelial inflammation and damage through the release of miRNA-loaded extracellular vesicles. We demonstrate that upon activation, neutrophils release EVs that are taken up by ECs, thus ensuring the transfer of miR-223, miR-142-3p and miR-451, three miRNAs that are normally expressed at very low levels in resting ECs.

While miR-223 has little effect on EC responses, we show that the induced expression of miR-142-3p and miR-451 in ECs results in profound endothelial damages, especially in pro-inflammatory conditions, characterized notably by a dramatic increase in cell apoptosis, impaired vascular repair responses, and induction of the secretion of pro-inflammatory chemokines and cytokines. We suggest that this process is particularly important in the pathophysiology of inflammatory diseases such as AAV, where neutrophils are strongly activated, release neutrophil extracellular traps (NETs) and thus get “trapped” in significant numbers in the microvasculature, resulting in a continuous local release and uptake by the endothelium of very high concentrations of EVs [26, 27]. In accordance with this model, we report that miR-223, miR-142-3p and miR-451 are high in kidney biopsies from patients with AAV, although this increase might reflect both the increased infiltration of leukocytes at the inflammatory site and the uptake of neutrophil-derived miRNA-loaded EVs by ECs.

The most striking effect of neutrophil-derived EVs in our model is the strong induction of EC apoptosis. Pro-apoptotic properties of EVs from different origins have been reported in several models, where it was shown to result from various processes, involving notably the generation of ROS [28]. Here, we show that the pro-apoptotic effect of neutrophil-derived EVs is mediated mostly through the transfer of miR-142-3p to targeted ECs. While miR-142-3p overexpression was found to induce apoptosis both in unstimulated and TNFα-stimulated ECs, we found that neutrophil-derived EVs were only able to induce significant apoptosis in the presence of TNFα. We suggest that this is due to the fact that miR-142-3p overexpression was very high in our overexpression model using miRNA mimics compared to the levels of miR-142-3p transferred through EVs in our co-incubation model.

Like most miRNAs, miR-142-3p has hundreds of mRNA targets, and its effects on EC responses are probably mediated through direct and indirect regulatory effects on a variety of genes and pathways. In this study, we demonstrate that one of its major effects in ECs is the inhibition of ERK1/2 and eNOS-mediated signals, two intracellular pathways that are essential for the maintenance of endothelial homeostasis [29, 30], and for the protection of EC from inflammation-induced apoptosis [31]. The blockade of these pathways by miR-142-3p may explain, at least in part, its strong apoptotic effect in the presence of TNFα. We also demonstrate that miR-142-3p inhibits the expression of RAC1, ROCK2 and CLIC4, three genes that are critical for EC migration and angiogenic responses [20-23]. This suggests that miR-142-3p abolishes vascular repair responses not only through induction of EC apoptosis, but also through the inhibition of EC migration.

Another consequence of the induced expression of miR-142-3p and miR-451 in EC is the induction of IL-6, IL-8, CXCL10 and CXCL11, four potent pro-inflammatory and leukocyte chemoattractant molecules. This suggests that the release of EVs by activated neutrophils may result in the triggering of an inflammatory cascade that will induce the recruitment at the inflammatory site of additional immune cells such as monocytes and T cells, thus resulting in the amplification and the maintenance of inflammation. However, inhibition of miR-142-3p and -451 in ECs using specific antagomirs did not prevent the release of IL-6, IL-8, CXCL10 and CXCL11 induced by EVs from activated neutrophils. This suggests that the transfer of miR-142-3p and -451 to ECs is not the main player in EVs pro-inflammatory effects and that additional mechanisms are involved. In fact, EVs are complex vessels that carry a variety of biologically active molecules such as nucleic acids, lipids and proteins and that can thus regulate a wide range of cellular responses through direct binding of cellular receptors or transfer of their various contents to the target cell. For instance, it has been shown that EVs from different origins can activate NF-κB signaling in ECs, thus resulting in endothelial activation and the secretion of IL-6 and IL-8 [32, 33]. This is therefore likely that different mechanisms contribute to EVs pro-inflammatory actions observed in our model.

While the induced expression of miR-142-3p and miR-451 in EC appears to have dramatic consequences for vascular integrity, miR-223 seems to have a rather protective effect in ECs. Indeed, we show that this miRNA accelerates vascular repair in wound-healing assays, and it was previously reported to inhibit the expression of tissue factor in ECs [34] and the induction of ICAM-1 expression upon TNFα stimulation [35]. Since this miRNA seems to be transferred in great quantity to EC through

neutrophil-derived EVs, this raises the question whether its expression might counterbalance the deleterious effects of miR-142-3p and miR-451. However, our co-incubation experiments demonstrate that neutrophil-derived EVs have an overall deleterious effect on ECs, characterized notably by a strong induction of apoptosis in the presence of TNFα, suggesting that the transfer of miR-223 is not sufficient to protect ECs from miR-142-3p and miR-451 induced injury.

The reason why neutrophils release EVs loaded with miR-223, -142-3p and -451 are elusive. These three miRNAs are known to be highly expressed in cells of the hematopoietic lineage [36], thus their release during neutrophil activation may be the result of a passive phenomenon due to their high intracellular concentration. However, a growing body of work shows that the release of miRNAs is a regulated active process and that the miRNA content of EVs is not random [37]. Thus, the loading of these miRNAs into EVs during neutrophil activation may be the result of an active mechanism that might participate in their pro-inflammatory response. For instance, miR-223 has been shown to downregulate neutrophil inflammatory responses, notably by inhibiting the formation of NETs [38]. miR-451 has also been shown to display anti-inflammatory effects through the down-regulation of neutrophil chemotaxis [39]. Therefore, the release of these miRNAs in response to pro-inflammatory stimuli might participate in the molecular mechanisms of neutrophil inflammatory responses.

Altogether, our studies unravel a new mechanism of neutrophil-induced vascular damage through the release and uptake of miR-142-3p and miR-451 loaded extracellular vesicles. Our findings suggest that this process may be critical in the pathogenesis of a number of inflammatory diseases besides ANCA-associated vasculitis, such as systemic lupus erythematosus and sepsis, which are characterized by a strong neutrophil activation and subsequent vascular damage. The main limitation of this study is the fact that this work was performed in an *in vitro* model of AAV, and the number of neutrophil-derived EVs applied to ECs was therefore somewhat arbitrary. Besides, our neutrophil isolation protocol excluded the subpopulation of low-density neutrophils (LDGs) that blend in the PBMC layer during ficoll purification [40]. However, while these LDGs have been shown to be markedly increased in patients with SLE and AAV and show enhanced capacity to synthesize type I IFNs and to form NETs, recent studies suggest that they display characteristics consistent with generic emergency granulopoïesis responders in the context of acute inflammation, rather than being primary drivers of AAV pathogenesis [41, 42]. Further *in vivo* studies in animal models will be

necessary to determine the importance of neutrophil-derived EVs in the development of vascular damage associated with AAV.

Micro-RNA targeting is an innovative therapeutic strategy that has shown great promises in preclinical studies and already reached clinical development in cancer and hepatitis C [43, 44]. Thus, the targeting of miR-142-3p and miR-451 in ECs, cells that normally express very little amounts of these two miRNAs at resting state, may have implications for the treatment of various neutrophil-mediated inflammatory vascular diseases.

Acknowledgements

We acknowledge the IBISA MicroPICell facility (Biogenouest), member of the national infrastructure France-Bioimaging supported by the French national research agency (ANR-10-INBS-04). This work was realized in the context of the IHU-Cesti project, which received French government financial support managed by the Agence Nationale de la Recherche via the Investments for the future program ANR-10-IBHU-005. The IHU-Cesti project is also supported by Nantes Metropole and the Pays de la Loire Region. This work was realized in the context of the LabEX IGO program supported by the Agence Nationale de la Recherche via the Investments for the future program ANR-11-LABX-0016-01. This work was supported by a grant from the Agence Nationale de la Recherche (ANR-15-CE14-0023), a Young Researcher Award from the Fondation du Rein and a fellowship grant from the Fondation pour la Recherche Médicale (FRM ARF20140129163) to Dr. Sarah Bruneau. This project has received funding from the European Union's Horizon 2020 research and innovation program under the Marie Sklodowska-Curie grant agreement No.660773.

Authorship contributions

A.G. participated in research design, performed the studies, analyzed and interpreted the data and participated in the writing of the manuscript. M.N., G.AG, B.M., R.LB and K.R. assisted with experiments. J.G., A.N., M.H. and F.F. provided scientific and clinical expertise and edited the manuscript. F.F. and S.B. initiated the research. S.B. conceived and designed the study, assisted with experiments and analyzes of data, and wrote the manuscript.

Disclosure statement

The authors have no conflicting financial interests to disclose.

REFERENCES

[1]. Raposo G., and Stoorvogel W., Extracellular vesicles: exosomes, microvesicles, and friends, The Journal of cell biology. 200 (2013) 373-83. https://doi.org/10.1083/jcb.201211138

[2]. Camussi G., Deregibus M.C., Bruno S., Cantaluppi V., and Biancone L., Exosomes/microvesicles as a mechanism of cell-to-cell communication, Kidney Int. 78 (2010) 838-48. https://doi.org/ki2010278 [pii]10.1038/ki.2010.278

[3]. Valadi H., Ekstrom K., Bossios A., Sjostrand M., Lee J.J., and Lotvall J.O., Exosome-mediated transfer of mRNAs and microRNAs is a novel mechanism of genetic exchange between cells, Nature cell biology. 9 (2007) 654-9. https://doi.org/10.1038/ncb1596

[4]. Creemers E.E., Tijsen A.J., and Pinto Y.M., Circulating microRNAs: novel biomarkers and extracellular communicators in cardiovascular disease?, Circ Res. 110 (2012) 483-95. https://doi.org/110/3/483 [pii]10.1161/CIRCRESAHA.111.247452

[5]. Martins V.R., Dias M.S., and Hainaut P., Tumor-cell-derived microvesicles as carriers of molecular information in cancer, Curr Opin Oncol. 25 (2013) 66-75. https://doi.org/10.1097/CCO.0b013e32835b7c81

[6]. Hsu Y.L., Hung J.Y., Chang W.A., Lin Y.S., Pan Y.C., Tsai P.H., et al., Hypoxic lung cancer-secreted exosomal miR-23a increased angiogenesis and vascular permeability by targeting prolyl hydroxylase and tight junction protein ZO-1, Oncogene. 36 (2017) 4929-42. https://doi.org/10.1038/onc.2017.105

[7]. Mao G., Liu Y., Fang X., Liu Y., Fang L., Lin L., et al., Tumor-derived microRNA-494 promotes angiogenesis in non-small cell lung cancer, Angiogenesis. 18 (2015) 373-82. https://doi.org/10.1007/s10456-015-9474-5

[8]. Umezu T., Tadokoro H., Azuma K., Yoshizawa S., Ohyashiki K., and Ohyashiki J.H., Exosomal miR-135b shed from hypoxic multiple myeloma cells enhances angiogenesis by targeting factor-inhibiting HIF-1, Blood. 124 (2014) 3748-57. https://doi.org/blood-2014-05-576116 [pii]10.1182/blood-2014-05-576116

[9]. Zhuang G., Wu X., Jiang Z., Kasman I., Yao J., Guan Y., et al., Tumour-secreted miR-9 promotes endothelial cell migration and angiogenesis by activating the JAK-STAT pathway, The EMBO journal. 31 (2012) 3513-23. https://doi.org/10.1038/emboj.2012.183

[10]. Mayadas T.N., Cullere X., and Lowell C.A., The multifaceted functions of neutrophils, Annual review of pathology. 9 (2014) 181-218. https://doi.org/10.1146/annurev-pathol-020712-164023

[11]. Eken C., Gasser O., Zenhaeusern G., Oehri I., Hess C., and Schifferli J.A., Polymorphonuclear neutrophil-derived ectosomes interfere with the maturation of monocyte-derived dendritic cells, J Immunol. 180 (2008) 817-24. https://doi.org/180/2/817 [pii]

[12]. Mesri M., and Altieri D.C., Endothelial cell activation by leukocyte microparticles, J Immunol. 161 (1998) 4382-7.

[13]. Mesri M., and Altieri D.C., Leukocyte microparticles stimulate endothelial cell cytokine release and tissue factor induction in a JNK1 signaling pathway, The Journal of biological chemistry. 274 (1999) 23111-8.

[14]. Daniel L., Fakhouri F., Joly D., Mouthon L., Nusbaum P., Grunfeld J.P., et al., Increase of circulating neutrophil and platelet microparticles during acute vasculitis and hemodialysis, Kidney Int. 69 (2006) 1416-23. https://doi.org/10.1038/sj.ki.5000306

[15]. Kettritz R., How anti-neutrophil cytoplasmic autoantibodies activate neutrophils, Clinical and experimental immunology. 169 (2012) 220-8. https://doi.org/10.1111/j.1365-2249.2012.04615.x

[16]. Hong Y., Eleftheriou D., Hussain A.A., Price-Kuehne F.E., Savage C.O., Jayne D., et al., Anti-neutrophil cytoplasmic antibodies stimulate release of neutrophil microparticles, Journal of

the American Society of Nephrology : JASN. 23 (2012) 49-62. https://doi.org/10.1681/ASN.2011030298

[17]. Van Der Geld Y.M., Limburg P.C., and Kallenberg C.G., Characterization of monoclonal antibodies to proteinase 3 (PR3) as candidate tools for epitope mapping of human anti-PR3 autoantibodies, Clinical and experimental immunology. 118 (1999) 487-96.

[18]. Billinge E.R., Broom M., and Platt M., Monitoring aptamer-protein interactions using tunable resistive pulse sensing, Analytical chemistry. 86 (2014) 1030-7. https://doi.org/10.1021/ac401764c

[19]. Livak K.J., and Schmittgen T.D., Analysis of relative gene expression data using real-time quantitative PCR and the 2(-Delta Delta C(T)) Method, Methods. 25 (2001) 402-8. https://doi.org/10.1006/meth.2001.1262

[20]. Bohman S., Matsumoto T., Suh K., Dimberg A., Jakobsson L., Yuspa S., et al., Proteomic analysis of vascular endothelial growth factor-induced endothelial cell differentiation reveals a role for chloride intracellular channel 4 (CLIC4) in tubular morphogenesis, The Journal of biological chemistry. 280 (2005) 42397-404. https://doi.org/10.1074/jbc.M506724200

[21]. Montalvo J., Spencer C., Hackathorn A., Masterjohn K., Perkins A., Doty C., et al., ROCK1 & 2 perform overlapping and unique roles in angiogenesis and angiosarcoma tumor progression, Current molecular medicine. 13 (2013) 205-19.

[22]. Tan W., Palmby T.R., Gavard J., Amornphimoltham P., Zheng Y., and Gutkind J.S., An essential role for Rac1 in endothelial cell function and vascular development, FASEB journal : official publication of the Federation of American Societies for Experimental Biology. 22 (2008) 1829-38. https://doi.org/10.1096/fj.07-096438

[23]. Soehnlein O., Steffens S., Hidalgo A., and Weber C., Neutrophils as protagonists and targets in chronic inflammation, Nature reviews Immunology. 17 (2017) 248-61. https://doi.org/10.1038/nri.2017.10

[24]. Mortaz E., Alipoor S.D., Adcock I.M., Mumby S., and Koenderman L., Update on Neutrophil Function in Severe Inflammation, Frontiers in immunology. 9 (2018) 2171. https://doi.org/10.3389/fimmu.2018.02171

[25]. Jennette J.C., Falk R.J., Hu P., and Xiao H., Pathogenesis of antineutrophil cytoplasmic autoantibody-associated small-vessel vasculitis, Annual review of pathology. 8 (2013) 139-60. https://doi.org/10.1146/annurev-pathol-011811-132453

[26]. Halbwachs L., and Lesavre P., Endothelium-neutrophil interactions in ANCA-associated diseases, Journal of the American Society of Nephrology : JASN. 23 (2012) 1449-61. https://doi.org/10.1681/ASN.2012020119

[27]. Kessenbrock K., Krumbholz M., Schonermarck U., Back W., Gross W.L., Werb Z., et al., Netting neutrophils in autoimmune small-vessel vasculitis, Nature medicine. 15 (2009) 623-5. https://doi.org/10.1038/nm.1959

[28]. Winberg L.K., Jacobsen S., and Nielsen C.H., Microparticles from patients with systemic lupus erythematosus induce production of reactive oxygen species and degranulation of polymorphonuclear leukocytes, Arthritis research & therapy. 19 (2017) 230. https://doi.org/10.1186/s13075-017-1437-3

[29]. Mavria G., Vercoulen Y., Yeo M., Paterson H., Karasarides M., Marais R., et al., ERK-MAPK signaling opposes Rho-kinase to promote endothelial cell survival and sprouting during angiogenesis, Cancer cell. 9 (2006) 33-44. https://doi.org/10.1016/j.ccr.2005.12.021

[30]. Siragusa M., and Fleming I., The eNOS signalosome and its link to endothelial dysfunction, Pflugers Archiv : European journal of physiology. 468 (2016) 1125-37. https://doi.org/10.1007/s00424-016-1839-0

[31]. Bulotta S., Barsacchi R., Rotiroti D., Borgese N., and Clementi E., Activation of the endothelial nitric-oxide synthase by tumor necrosis factor-alpha. A novel feedback mechanism regulating cell death, The Journal of biological chemistry. 276 (2001) 6529-36. https://doi.org/10.1074/jbc.M006535200

[32]. Tang N., Sun B., Gupta A., Rempel H., and Pulliam L., Monocyte exosomes induce adhesion molecules and cytokines via activation of NF-kappaB in endothelial cells, FASEB journal : official publication of the Federation of American Societies for Experimental Biology. 30 (2016) 3097-106. https://doi.org/10.1096/fj.201600368RR

[33]. Atehortua L., Rojas M., Vasquez G., Munoz-Vahos C.H., Vanegas-Garcia A., Posada-Duque R.A., et al., Endothelial activation and injury by microparticles in patients with systemic lupus erythematosus and rheumatoid arthritis, Arthritis research & therapy. 21 (2019) 34. https://doi.org/10.1186/s13075-018-1796-4

[34]. Li S., Chen H., Ren J., Geng Q., Song J., Lee C., et al., MicroRNA-223 inhibits tissue factor expression in vascular endothelial cells, Atherosclerosis. 237 (2014) 514-20. https://doi.org/10.1016/j.atherosclerosis.2014.09.033

[35]. Li J., Tan M., Xiang Q., Zhou Z., and Yan H., Thrombin-activated platelet-derived exosomes regulate endothelial cell expression of ICAM-1 via microRNA-223 during the thrombosis-inflammation response, Thrombosis research. 154 (2017) 96-105. https://doi.org/10.1016/j.thromres.2017.04.016

[36]. Merkerova M., Belickova M., and Bruchova H., Differential expression of microRNAs in hematopoietic cell lineages, European journal of haematology. 81 (2008) 304-10. https://doi.org/10.1111/j.1600-0609.2008.01111.x

[37]. O'Brien K., Breyne K., Ughetto S., Laurent L.C., and Breakefield X.O., RNA delivery by extracellular vesicles in mammalian cells and its applications, Nature reviews Molecular cell biology. 21 (2020) 585-606. https://doi.org/10.1038/s41580-020-0251-y

[38]. Liao T.L., Chen Y.M., Tang K.T., Chen P.K., Liu H.J., and Chen D.Y., MicroRNA-223 inhibits neutrophil extracellular traps formation through regulating calcium influx and small extracellular vesicles transmission, Scientific reports. 11 (2021) 15676. https://doi.org/10.1038/s41598-021-95028-0

[39]. Murata K., Yoshitomi H., Furu M., Ishikawa M., Shibuya H., Ito H., et al., MicroRNA-451 down-regulates neutrophil chemotaxis via p38 MAPK, Arthritis & rheumatology. 66 (2014) 549-59. https://doi.org/10.1002/art.38269

[40]. Carmona-Rivera C., and Kaplan M.J., Low-density granulocytes: a distinct class of neutrophils in systemic autoimmunity, Seminars in immunopathology. 35 (2013) 455-63. https://doi.org/10.1007/s00281-013-0375-7

[41]. Ui Mhaonaigh A., Coughlan A.M., Dwivedi A., Hartnett J., Cabral J., Moran B., et al., Low Density Granulocytes in ANCA Vasculitis Are Heterogenous and Hypo-Responsive to Anti-Myeloperoxidase Antibodies, Frontiers in immunology. 10 (2019) 2603. https://doi.org/10.3389/fimmu.2019.02603

[42]. Jones B.E., Herrera C.A., Agosto-Burgos C., Starmer J., Bass W.A., Poulton C.J., et al., ANCA autoantigen gene expression highlights neutrophil heterogeneity where expression in normal-density neutrophils correlates with ANCA-induced activation, Kidney Int. 98 (2020) 744-57. https://doi.org/10.1016/j.kint.2020.04.037

[43]. Janssen H.L., Reesink H.W., Lawitz E.J., Zeuzem S., Rodriguez-Torres M., Patel K., et al., Treatment of HCV infection by targeting microRNA, The New England journal of medicine. 368 (2013) 1685-94. https://doi.org/10.1056/NEJMoa1209026

[44]. Rupaimoole R., and Slack F.J., MicroRNA therapeutics: towards a new era for the management of cancer and other diseases, Nature reviews Drug discovery. 16 (2017) 203-22. https://doi.org/10.1038/nrd.2016.246

FIGURE LEGENDS

Figure 1. Neutrophil activation induces the release of extracellular vesicles that ensure the transfer of miR-223, miR-142-3p and miR-451 to microvascular endothelial cells.

Neutrophils from healthy volunteers were primed for 15 min with 2 ng/mL of TNFα, and subsequently activated with 5 µg/mL of mouse monoclonal anti-PR3 IgG1 (clone CLB12.8) for 4 hours. EVs released in the culture medium were isolated using the Exoquick™ Reagent. (**A**) EVs released by anti-PR3 activated neutrophils and unactivated neutrophils were analyzed by tunable resistive pulse sensing (TRPS, qNano, IZON). Representative diagrams of size distribution obtained with the NP100 (left) and NP400 nanopores (right) are shown (from n=4 experiments). pt = particle. (**B-C**) Mean concentration and size diameter of neutrophil-derived EVs (±SEM) from 4 independent experiments. (**D**) EVs released by anti-PR3 activated neutrophils were stained with the lipophilic red fluorescent dye Vybrant® DiD and co-incubated for 3 hrs and 24 hrs with HDMEC. The cell membrane of HDMEC is visualized with a CD31 staining (in green), and their nuclei with DAPI (in blue). EV uptake by HDMEC was visualized by confocal microscopy on a Nikon Eclipse T1 microscope and the Nikon NIS-Elements software (X60 magnification). Representative images from n=3 experiments are shown. An orthogonal view is illustrated at 24 hrs and shows that EV are localized inside the cytoplasm of HDMEC, under the plasma membrane. (Scale bars: 25 µm) (**E**) Representative dot plot from n=3 flow cytometry analyzes of HDMEC co-incubated for 24 hrs with labelled EV, showing that most of the cells (here 93.1%) have taken up neutrophil-derived EVs. (**F**) qPCR analyzes of the expression of miR-223, miR- 142-3p and miR-451 in HDMEC co-incubated for 24 hrs with EVs released by anti-PR3 activated neutrophils (+EV) vs. resting HDMEC (NT). The scatter plots represent each individual value and the mean fold change (± SEM) in the expression of the mature (black dots) and primary forms (grey dots) of these miRNAs, from five independent experiments. (**G**) qPCR analyzes of the expression of miR-223, miR-142-3p and miR-451 in HDMEC co-incubated for 24 hrs with EVs released by neutrophils from healthy volunteers upon their activation with 200 µg/mL of IgG purified from the plasma of patients with anti-PR3 ANCA (AAV-IgG), 1 µM fMLP, 20 nM PMA, or 100 ng/mL LPS. The scatter plots represent individual values and the mean fold change (± SEM) in miRNA expression vs. untreated HDMEC (No EV) from n ≥ 3 independent experiments. **P*<0.05, ***P*<0.01, ****P*<0.001.

Figure 2. miR-142-3p and miR-451 induce profound microvascular endothelial cell damage.

HDMEC were transfected with 10 nM of mimics of miR-223, miR-142-3p, miR-451 or a negative control mimic, and TNFα (100 U/mL) was added to the culture medium 24 hours after transfection. Cell responses were evaluated at 48 hours after transfection: (**A**) HDMEC apoptosis was analyzed by flow cytometry using Annexin V stainings. The scatter plot represents the percentages (and mean ± SEM) of apoptotic cells (Annexin V+) from 8 independent experiments. (**B**) HDMEC proliferation was assessed by analyzing by flow cytometry the percentage of cells that incorporated BrdU during the last 24 hours of cell culture. The scatter plot represents the percentages of proliferative cells (BrdU+) from 8 independent experiments (with mean ± SEM). (**C**) A linear "scratch" was created in HDMEC monolayers 48 hours after mimic transfection, and the migration of cells into this wound was measured after 24 additional hours of cell culture. Representative photomicrographs (10X magnification) of wounds at 0 hr and after 24 hrs are shown, the white lines highlighting the wound for each group of cells (Scale bars: 200 µm). The scatter plot shows the percentages of wound closure from 6 independent experiments (with mean ± SEM). (**D**) HDMEC were seeded on top of a Matrigel matrix and cultured for an additional 6 hours to allow the formation of tube-like structures. A representative photomicrograph of each condition is shown (40X ; Scale bars: 200 µm), and the scatter plot shows quantitative analysis of the mean number of junctions between tubes per field (four fields per condition) (± SEM), from 7 independent experiments. **P*<0.05, ****P*<0.001.

Figure 3. miR-142-3p inhibits critical genes and pathways in microvascular endothelial cells.

HDMEC were transfected with 10 nM of a miR-142-3p mimic or a negative control mimic, 100 U/mL of TNFα was added to the culture medium 24 hours after transfection, and analyzes were performed after an additional 24 hours of cell culture. (**A**) The expression of phospho-eNOS (S1177), total eNOS, phospho-ERK1/2 (T202/Y204), total ERK1/2 and β-actin was analyzed by Western blot. Representative results of ≥2 independent experiments are shown. Scatter plots represent the quantification of protein bands by densitometry, expressed as the ratio of phosphorylated eNOS / total eNOS (top graph) and of phosphorylated ERK1/2 / total ERK1/2 (lower graph) (with mean ± SEM). (**B**) The mRNA expression of RAC1, ROCK2 and CLIC4 were analyzed by qPCR. Scatter plots show the

fold changes in mRNA expression (with mean ± SEM) from 5 independent experiments. *P<0.05, **P<0.01, ***P<0.001.

Figure 4. miR-142-3p and miR-451 induce the expression of pro-inflammatory cytokines and chemokines by microvascular endothelial cells but are not the sole players of EV-induced inflammation.

(**A**) HDMEC were transfected with 10 nM of mimics of miR-142-3p and miR-451, or a negative control mimic (CT). The mRNA expression of IL-6, IL-8, CXCL10 and CXCL11 was analyzed by qPCR forty-eight hours after transfection. Scatter plots show the fold changes in mRNA expression (with mean ± SEM), from ≥6 independent experiments. (**B**) IL-6, IL-8, CXCL10 and CXCL11 protein expressions were analyzed by ELISA in the culture supernatant of HDMEC afeter 48 hrs of co-incubation with EVs released by neutrophils activated with IgG from patients with PR3-AAV (EV-PR3 IgG) or by resting neutrophils (EV NS). Scatter plots represent the concentrations (pg/mL) of each molecule (with mean ± SEM) from 5 independent experiments. (**C**) HDMEC were transfected with 20 nM of specific miR-142-3p and miR-451 inhibitors (antagomiR), or a negative control antagomiR, and EVs released by PR3 ANCA-activated neutrophils were added to the culture medium 24 hours later. After an additional 24 hrs of culture, IL-6, IL-8, CXCL10 and CXCL11 release was quantified in the culture supernatant by ELISA. The scatter plots represent the concentrations (pg/mL) of each molecule (with mean ± SEM) from 6 independent experiments. *P<0.05, **P<0.01.

Figure 5. Extracellular vesicles released by ANCA-activated neutrophils induce microvascular EC apoptosis in the presence of TNFα through miR-142-3p-dependent mechanisms.

(**A**) Neutrophils from healthy volunteers were primed with 2 ng/mL of TNFα for 15 minutes, and further activated with 5 µg/mL of murine monoclonal anti-PR3 IgG1 (clone PR3-G2). EVs released in the culture supernatant of these activated neutrophils or from neutrophils cultured for four hours without stimulation (“resting neutrophils”, NS) were isolated using the Exoquick™ reagent. HDMEC were co-incubated for 72 hours with these EVs, in the presence or absence of 100 U/mL TNFα, and apoptosis was assessed by flow cytometry using Annexin V staining. The scatter plot shows the percentages of apoptotic HDMEC (Annexin V+) for each condition from 3 independent experiments (with mean ±

SEM). (**B**) HDMEC were transfected with 20 nM of specific miR-142-3p and miR-451 inhibitors (antagomiR), or a negative control antagomiR and 24 hrs later, EVs released by neutrophils activated with a murine monoclonal anti-PR3 IgG1 (clone PR3-G2) were added to the culture medium. HDMEC apoptosis was evaluated after additional 48 hrs of culture. The scatter plots represent the percentages of apoptotic HDMEC (Annexin V+) for each condition (with mean ± SEM) from n=5 independent experiments. **P*<0.05, ***P*<0.01.

Figure 6. miR-223, miR-142-3p and miR-451 are augmented in kidney biopsies from patients with ANCA-associated vasculitis.

miR-223, miR-142-3p and miR-451 levels were measured by qPCR in kidney biopsies from eight patients with ANCA-associated vasculitis, five patients with a control non-proliferative glomerulonephritis (minimal change diseases (black dots) and membranous nephropathy (empty black dot)), and nine patients with other proliferative glomerulonephritides (lupus nephritis (squares), membranoproliferative glomerulonephritis (diamond) and IgA nephropathy (inverted triangles)). Patients under immunosuppressive therapy are shown in red and patients without treatment at the time of biopsy are shown in black. Patients' clinical characteristics are gathered in **Tables 1 and 2**. The graphs illustrate the fold change in each miRNA expression (with mean ± SEM). **P*<0.05, ***P*<0.01.

Age (yrs)	Sex	ANCA subtype	Diagnosis	Context	BVAS	ANCA titer (xULN)	Hematuria	Proteinuria (uPCR, g/g)	CRP (mg/L)	eGFR (ml/min/1.73 m²)	% abnormal glomeruli	Extrarenal involvement						miRNA expression (fold change)		
												ENT	Lung	Skin	Nerve	A/M	Const.	miR-223	miR-142-3p	miR-451
18	F	MPO	MPA	Newly diagnosed, untreated	12	1.1	++	0.95	50	63	50	0	0	1	0	0	0	1.80	3.22	14.29
75	F	MPO	MPA	1st relapse, off therapy	30	26.8	+++	3.4	140	16	34	0	DAH	1	1	1	0	5.77	6.39	1.54
66	F	PR3	GPA	Newly diagnosed, untreated	25	25	+++	0.55	126	36	33	1	Nod	0	0	1	1	2.83	2.20	4.46
78	F	MPO	MPA	Newly diagnosed, untreated	12	5.6	+++	0.99	42	11	76	0	0	0	0	0	0	2.26	2.64	0.55
67	M	PR3	GPA	Newly diagnosed, untreated	23	31	+++	1.38	85	6	100	1	0	1	0	1	1	2.36	1.01	1.42
59	M	MPO	MPA	Newly diagnosed, untreated	17	26.8	+	0.45	114	15	50	0	Nod	1	0	1	1	4.12	1.37	0.41
65	M	PR3	GPA	Newly diagnosed, untreated	13	22.6	+++	0.6	60	128	24	1	DAH	1	0	0	1	0.64	0.29	0.20
57	M	MPO	MPA	Newly diagnosed, untreated	26	7	++	3.6	127	7	90	1	DAH	0	0	0	1	0.96	0.56	0.08

Table 1: Clinical and biological characteristics of patients with ANCA-Associated Vasculitis

*MPO: myeloperoxidase, PR3: proteinase 3, MPA: microscopic polyangiitis, GPA: granulomatosis with polyangiitis, BVAS: Birmingham Vasculitis Activity Score, uPCR: urine protein/creatinine ratio, CRP: C-reactive protein, eGFR: estimated glomerular filtration rate (CKD-EPI), ENT: ear-nose-throat, DAH: diffuse alveolar hemorrhage, Nod: nodules, A/M: arthralgia/myalgia, Const.: constitutional symptoms (fever, weight loss)

	Age	Sex	Diagnosis	Treatment	Proteinuria (uPCR, g/g)	eGFR (ml/min/1.73m²)
Proliferative GN	48	M	SLE-GN, Class III	HCQ, Cs	5.7	117
	42	F	SLE-GN, Class IV	MTX, Cs	2.4	100
	32	F	SLE-GN, Class IV	HCQ, Cs	1.6	117
	21	F	SLE-GN, Class IV	HCQ, MTX, Cs	0.7	91
	43	F	SLE-GN, Class IV	None	3.5	60
	76	F	Cryo-MPGN	None	0.7	42
	27	F	IgA-Vas	None	1.7	104
	65	M	IgA-GN	None	0.6	29
	76	F	IgA-GN	None	2.3	18
Non-proliferative GN	25	F	MCD	None	7.5	122
	77	M	MCD	None	8.8	62
	19	M	MCD	None	13	131
	52	M	MCD	None	3	57
	63	F	pMN	None	3.5	93

Table 2: Clinical and biological characteristics of control patients with proliferative and non-proliferative glomerulonephritis

* Cryo: cryoglobulinemia, Cs: corticosteroids, eGFR: estimated glomerular filtration rate (CKD-EPI), GN: glomerulonephritis, HCQ: hydroxychloroquine, Vas: vasculitis, MCD: minimal change disease, MPGN: membranoproliferative glomerulonephritis, pMN: primary membranous nephropathy, MTX: methotrexate, SLE: systemic lupus erythematosus, uPCR: urine protein/creatinine ratio.

FIGURE 1

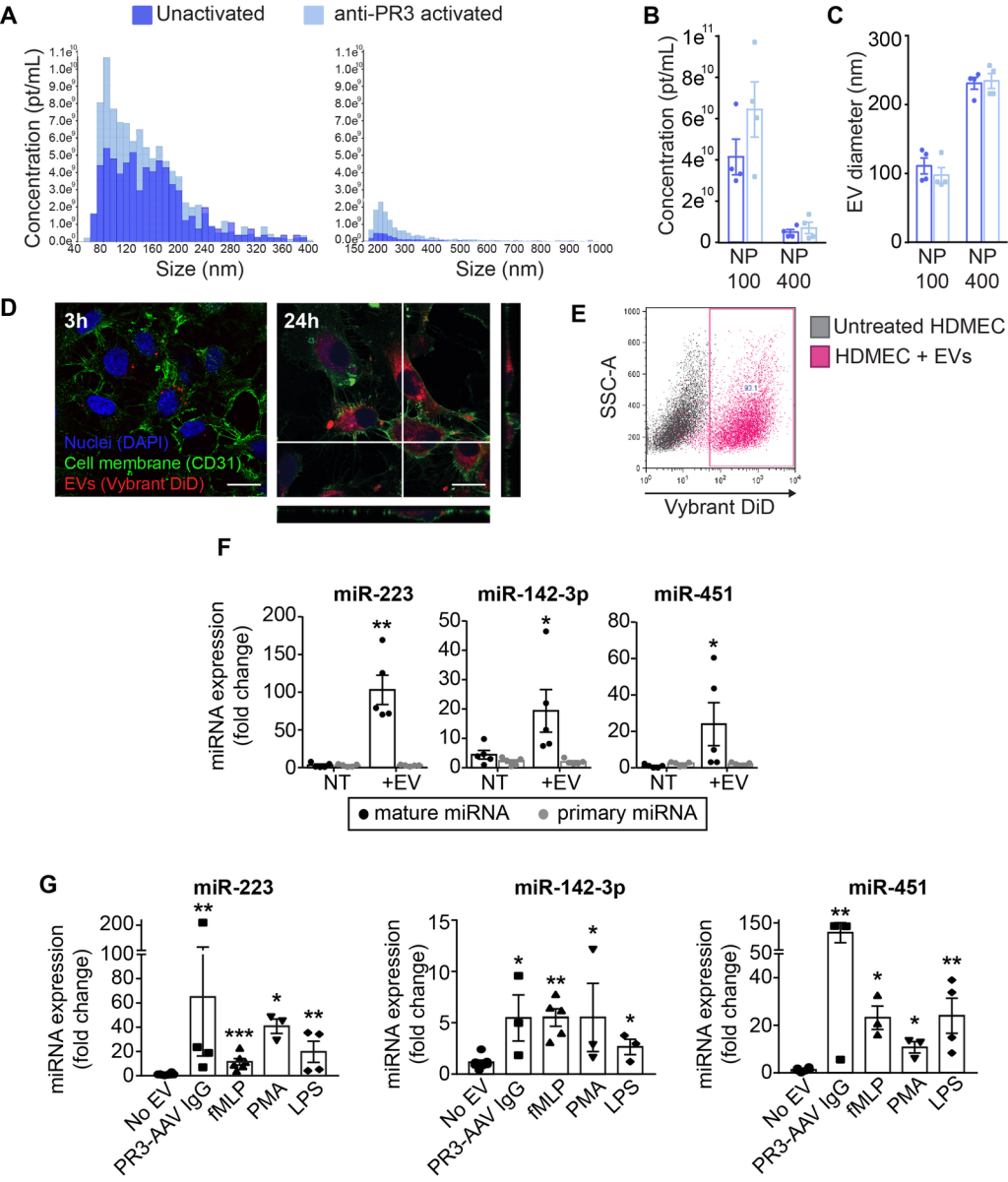
A
Unactivated
anti-PR3 activated
Concentration (pt/mL)
Size (nm)
B
Concentration (pt/mL)
NP 100
NP 400
C
EV diameter (nm)
NP 100
NP 400
D
3h
24h
Nuclei (DAPI)
Cell membrane (CD31)
EVs (Vybrant DiD)
E
Untreated HDMEC
HDMEC + EVs
SSC-A
Vybrant DiD
F
miR-223
miR-142-3p
miR-451
miRNA expression (fold change)
NT
+EV
mature miRNA
primary miRNA
G
miR-223
miR-142-3p
miR-451
miRNA expression (fold change)
No EV
PR3-AAV IgG
fMLP
PMA
LPS

FIGURE 2

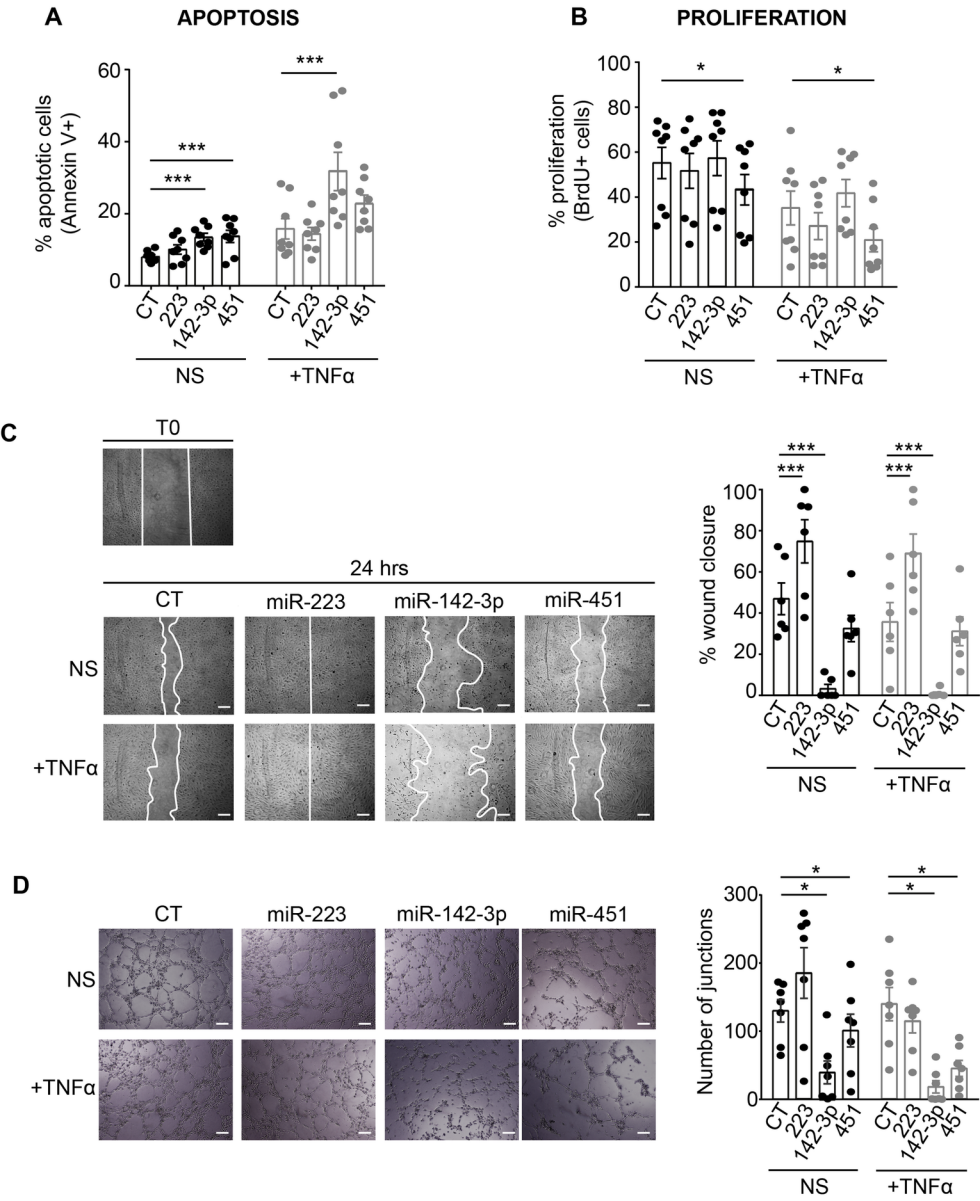
A
APOPTOSIS
% apoptotic cells (Annexin V+)
60
40
20
0
***
***
***
CT
223
142-3p
451
NS
+TNFα
B
PROLIFERATION
% proliferation (BrdU+ cells)
100
80
60
40
20
0
*
*
CT
223
142-3p
451
NS
+TNFα
C
T0
24 hrs
CT
miR-223
miR-142-3p
miR-451
NS
+TNFα
% wound closure
100
80
60
40
20
0
***
***
***
***
CT
223
142-3p
451
NS
+TNFα
D
CT
miR-223
miR-142-3p
miR-451
NS
+TNFα
Number of junctions
300
200
100
0
*
*
*
*
CT
223
142-3p
451
NS
+TNFα

FIGURE 3

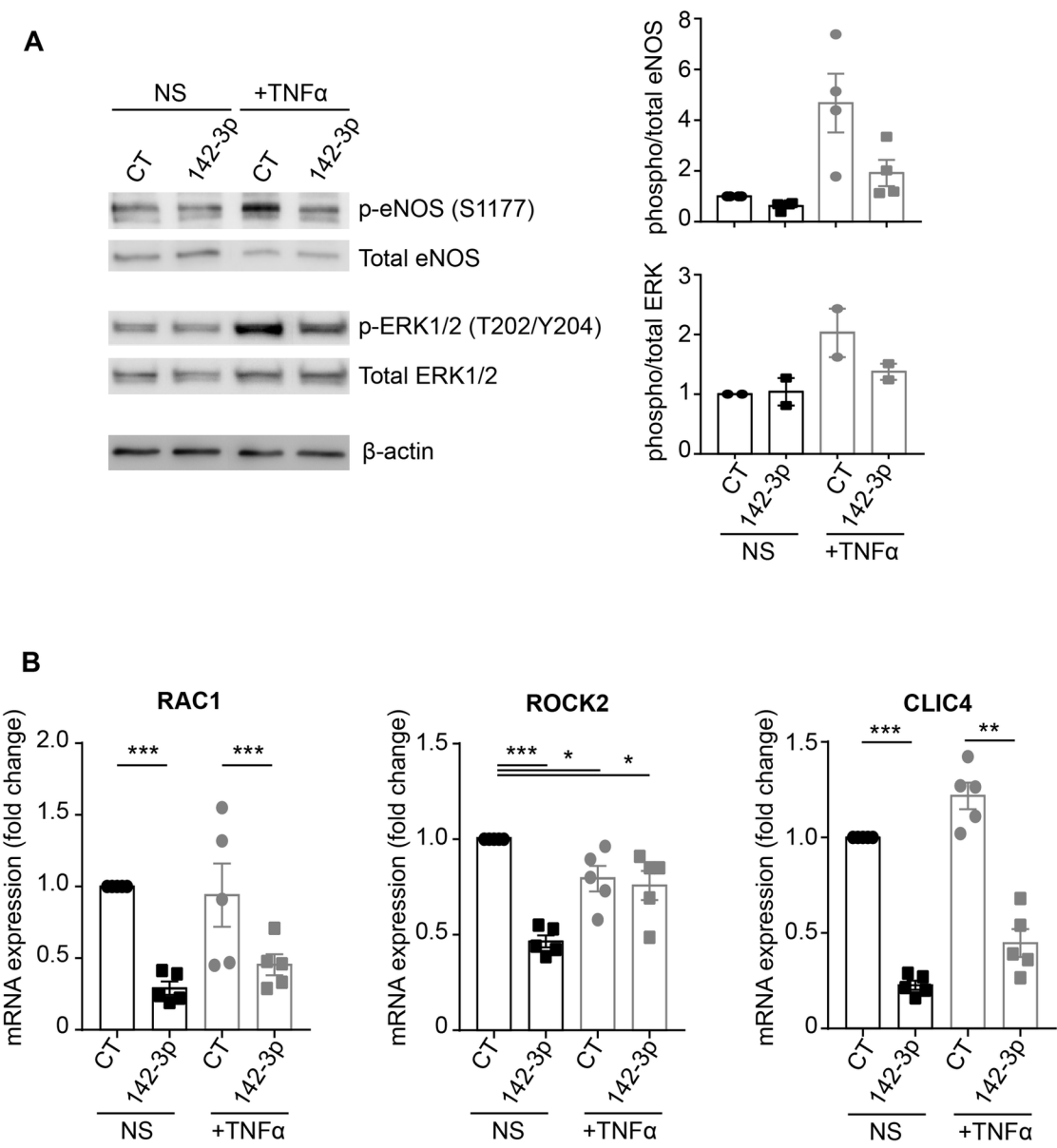
A
NS
+TNFα
CT
142-3p
CT
142-3p
p-eNOS (S1177)
Total eNOS
p-ERK1/2 (T202/Y204)
Total ERK1/2
β-actin
phospho/total eNOS
phospho/total ERK
CT
142-3p
CT
142-3p
NS
+TNFα
B
RAC1
ROCK2
CLIC4
mRNA expression (fold change)
***
***
***
*
*
***
**
CT
142-3p
CT
142-3p
NS
+TNFα

FIGURE 4

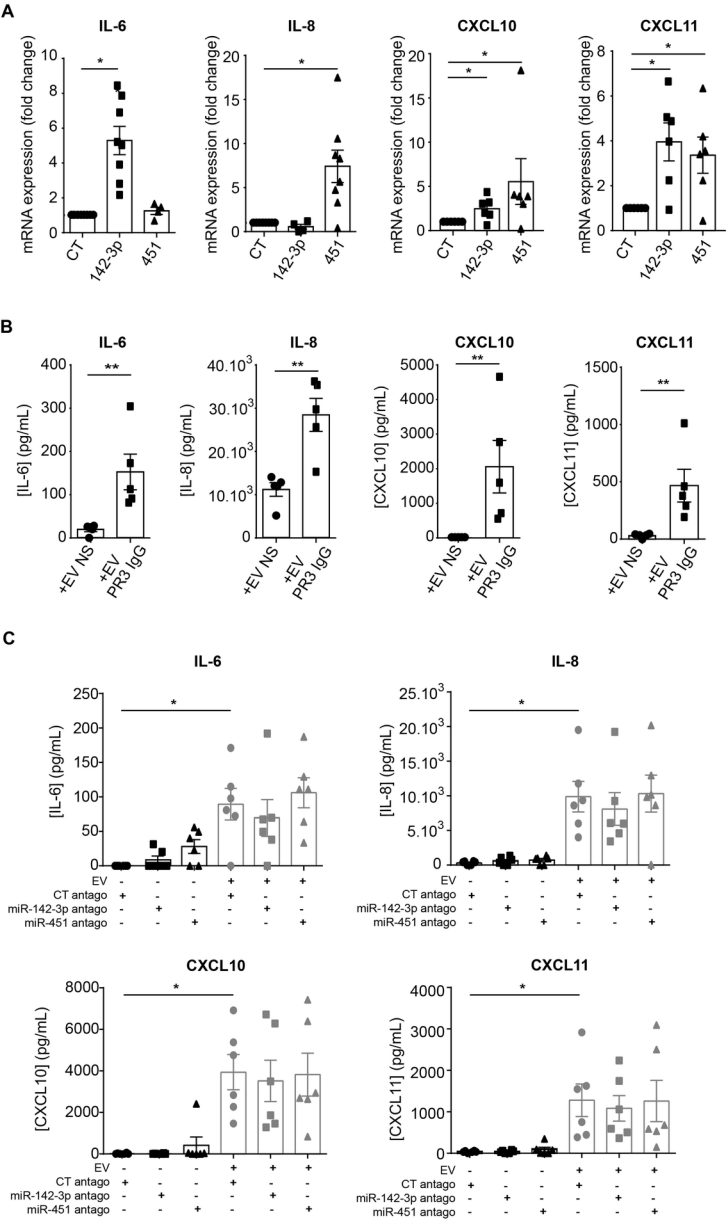
A
IL-6
IL-8
CXCL10
CXCL11
mRNA expression (fold change)
CT
142-3p
451
B
IL-6
IL-8
CXCL10
CXCL11
[IL-6] (pg/mL)
[IL-8] (pg/mL)
[CXCL10] (pg/mL)
[CXCL11] (pg/mL)
+EV NS
+EV PR3 IgG
C
IL-6
IL-8
CXCL10
CXCL11
[IL-6] (pg/mL)
[IL-8] (pg/mL)
[CXCL10] (pg/mL)
[CXCL11] (pg/mL)
EV
CT antago
miR-142-3p antago
miR-451 antago

FIGURE 5

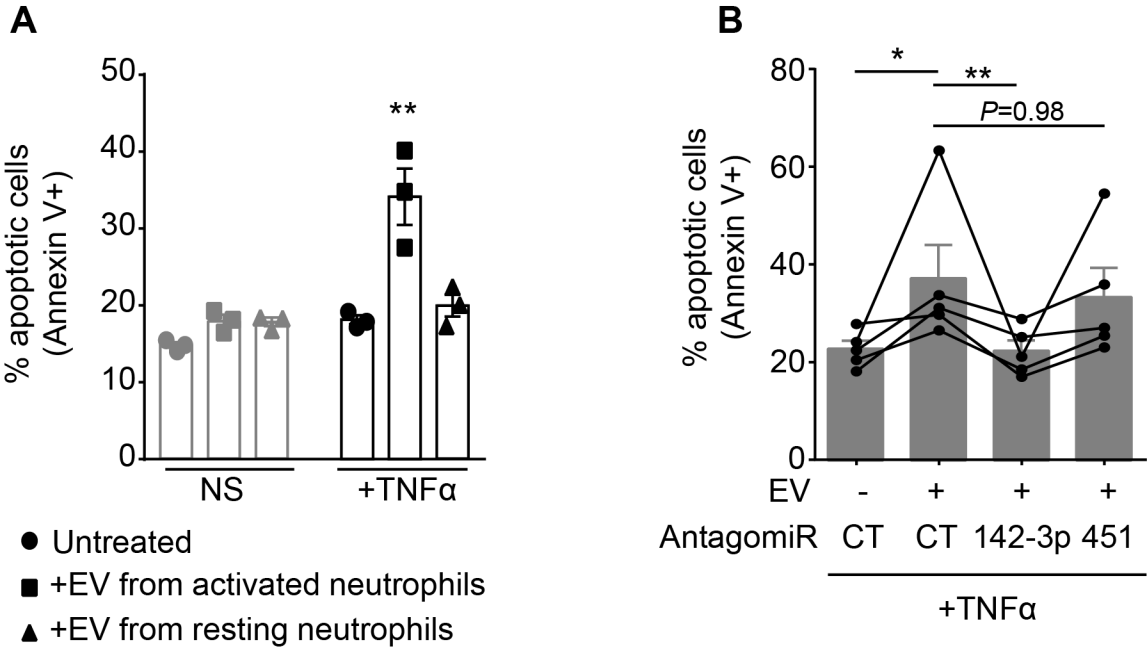
A
50
40
30
20
10
0
% apoptotic cells (Annexin V+)
**
NS
+TNFα
● Untreated
■ +EV from activated neutrophils
▲ +EV from resting neutrophils
B
80
60
40
20
0
% apoptotic cells (Annexin V+)
*
**
P=0.98
EV - + + +
AntagomiR CT CT 142-3p 451
+TNFα

FIGURE 6

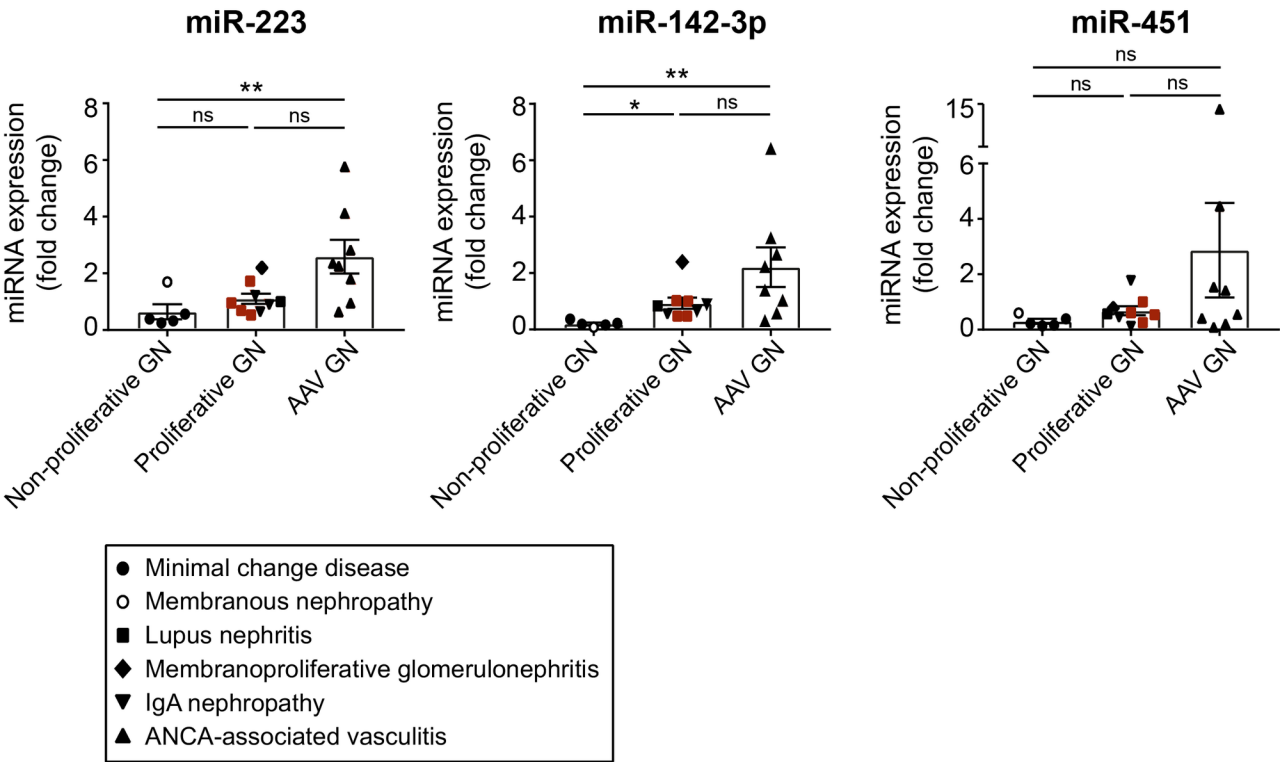
miR-223
miR-142-3p
miR-451
miRNA expression (fold change)
**
*
ns
Non-proliferative GN
Proliferative GN
AAV GN
Minimal change disease
Membranous nephropathy
Lupus nephritis
Membranoproliferative glomerulonephritis
IgA nephropathy
ANCA-associated vasculitis